(Memo)
594

DEC[redacted]ED 62 ~~79984~~

NASA TM X-160

NASA TM X-160

TECHNICAL MEMORANDUM
X-160

EFFECTS OF BOUNDARY-LAYER SUCTION AND SPOILERS ON TRANSONIC FLUTTER DERIVATIVES FOR A MIDSPAN CONTROL SURFACE ON AN UNSWEPT WING

By John A. Wyss, Robert E. Dannenberg,
Robert M. Sorenson, and Bruno J. Gambucci

Ames Research Center
Moffett Field, Calif.

Declassified by authority of NASA
Classification Change Notices No. ___
Dated ** 6/23/66

DECLASSIFIED- AUTHORITY
US: 1286 DROBKA TO LEBOW
MEMO DATED
6/8/66

[redacted]

FACILITY FORM 602

N66 33315	
(ACCESSION NUMBER)	(THRU)
29	1
(PAGES)	(CODE)
TMX-160	01
(NASA CR OR TMX OR AD NUMBER)	(CATEGORY)

GPO PRICE $ ______

CFSTI PRICE(S) $ ______

Hard copy (HC) 2.00

Microfiche (MF) .50

ff 653 July 65

NATIONAL AERONAUTICS AND SPACE ADMINISTRATION

WASHINGTON February 1960

[redacted]

NATIONAL AERONAUTICS AND SPACE ADMINISTRATION

TECHNICAL MEMORANDUM X-160

EFFECTS OF BOUNDARY-LAYER SUCTION AND SPOILERS ON TRANSONIC FLUTTER DERIVATIVES FOR A MIDSPAN CONTROL SURFACE ON AN UNSWEPT WING*

By John A. Wyss, Robert E. Dannenberg,
Robert M. Sorenson, and Bruno J. Gambucci

SUMMARY

The effects of suction and spoilers on transonic sectional control-surface flutter derivatives were determined in the Ames 14-foot transonic wind tunnel for a midspan flap-type control surface on a straight wing having an aspect ratio of 3, a taper ratio of 0.6, and a wing-thickness ratio of 0.06. Flap chord extended from the 70-percent chord station to the trailing edge. Suction was applied on spanwise perforated strips on each side of the control surface for successive locations of 77.3-, 86.6-, and 95.7-percent wing chord. The spoilers were 0.3 inch high, corresponding to a height to midspan wing chord ratio of 0.006 and were located on the control at the 82-percent wing chord station.

The application of suction during control-surface oscillation reduced the damping at subsonic speeds and lowered the Mach number for instability. In contrast, the spoilers had a stabilizing effect at subsonic speeds.

INTRODUCTION

Recent studies of the single-degree-of-freedom (rotational) flutter of flap-type control surfaces have indicated that unless the designer resorts to the addition of nonaerodynamic damping, this type of flutter cannot be prevented in limited transonic speed ranges except by a change in the configuration. Examples of such a configuration change, given in references 1 through 4, include a solid wedge type control surface with a blunt trailing edge, addition of triangular wedges (tetrahedra), use of spoilers on the control surface, or simply reduction of control-surface aspect ratio. Each of these modifications was found to reduce or eliminate flutter over certain speed ranges; however, such changes in

---

*Title, Unclassified

configuration except for the latter would be expected to produce undesirable drag penalties (e.g., ref. 5).

A means of influencing the flow field without changing the profile, and thus possibly avoiding a drag penalty, is the use of suction on or near the control surface. It was reasoned that suction would influence the shock wave and the boundary layer and hence would affect aerodynamic damping of the surface. An exploratory program was conducted to determine the effects on transonic flutter derivatives of suction applied on single spanwise strips on both sides of a conventional flap-type control surface. The strips were tested for three successive chordwise stations. In addition, the effect of spoilers mounted on the control surface was investigated. The results for such a spoiler configuration on a swept wing are contained in reference 4.

The control surface tested was a midspan 30-percent plain flap which formed part of a 6-percent-thick unswept wing with an aspect ratio of 3. The sectional flutter derivatives were determined by means of pressure cells at forced frequencies of the control surface from 10 to 30 cycles per second for a constant amplitude of $\pm 1.08^{\circ}$. Mach number varied from 0.6 to 1.12, with corresponding Reynolds number ranging from 10.4 to 14.8×10^{6}. Angle of attack and mean angle of flap deflection were 0°.

NOTATION

b local wing semichord, ft

c_b balance chord (distance from hinge line to leading edge of control), ft

c_f control chord (distance from hinge line to trailing edge), ft

c_h control hinge-moment coefficient, $\dfrac{HM}{\frac{1}{2}\rho V^2 c_t{}^2}$

c_{h_δ} $\dfrac{\partial c_h}{\partial \delta}$, per radian

$c_{h_{\dot{\delta}}}$ aerodynamic damping-moment coefficient, $\dfrac{\partial c_h}{\partial\left(\frac{\dot{\delta} b}{V}\right)}$

c_p pressure coefficient, $\dfrac{p_l - p}{q}$

c_q suction quantity coefficient, $\dfrac{Q}{VS_s}$

c_t total-control chord, $c_b + c_f$, ft

f frequency, cps

HM hinge moment, foot-pounds per foot of span

k reduced frequency, $\frac{\omega b}{V}$, with b taken at 3/8 semispan

M free-stream Mach number

p_l local static pressure, lb/ft^2

p free-stream static pressure, lb/ft^2

q free-stream dynamic pressure, lb/ft^2

Q quantity flow rate of suction air, ft^3/sec

S_s suction reference area, portion of wing area included within flap span, ft^2 (see fig. 4)

V velocity of air stream, ft/sec

x longitudinal distance in chord lengths

α angle of attack, deg

δ control-surface deflection angle, radians except where noted

δ_m mean angle of control-surface deflection, deg

$\dot{\delta}$ control-surface angular velocity, $\frac{d\delta}{dt}$, radians/sec

θ phase angle of resultant aerodynamic moment with respect to control-surface displacement, deg

ρ density of air stream, $slugs/ft^3$

ω angular frequency, $2\pi f$, radians/sec

Vector Notation

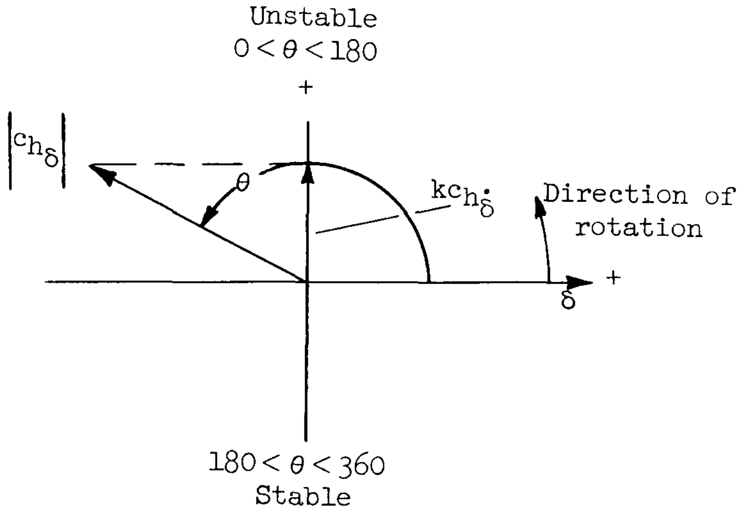

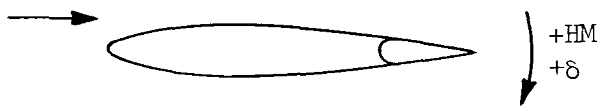

APPARATUS

The present investigation was conducted in the Ames 14-foot transonic wind tunnel. Descriptions of this tunnel and the apparatus used therein, the control-surface drive system, instrumentation, and corrections and precision applicable to the measurement technique are contained in reference 2. A sectional sketch of the nozzle and test section is shown in figure 1. Figure 2 shows a view of the model mounted in the test section. A schematic drawing of the control-surface drive system is shown in figure 3.

Model

The model (fig. 2) was mounted on base plates bolted to the tunnel floor. Model plan-form dimensions are shown in figure 4. The basic model is a wing with an aspect ratio of 3, a 6-foot semispan, a taper ratio of 0.6, an unswept 70-percent chord line, and a 30-percent-chord trailing-edge-type flap occupying the middle half of the semispan. The wing had an NACA 65A006 profile which was modified to a blunt trailing edge of 0.2-inch thickness. This modification facilitated pressure-cell installation at the trailing edge. Chordwise rows of pressure cells and pressure orifices were installed at 3/8 and 5/8 stations of the semispan. The control surface had a balance-chord to flap-chord ratio of 0.25 based on the mean aerodynamic chord of the flap. The hinge line was perpendicular to the wind stream.

Previous experience indicated the necessity for additional stiffness and damping of the wing. This was provided by a 5/32-inch aircraft cable which was passed through the plastic wing tip, sweptback about 20°, and attached to a cantilever spring system outside the tunnel walls (see fig. 2). It was found that the control surface could be oscillated safely, with negligible coupling between the control surface and wing.

Control Surface and Suction System

A typical cross-section drawing of the model is shown in figure 5. The spar of the wing was constructed of steel plates in order to provide ducting between the vacuum pumps and the control surface.

The porous skin of the control surface, shown in figure 6, consisted of a perforated aluminum sheet fastened to ribs which were spaced approximately 6 inches apart. The perforated sheet (0.125 inch thick) had 47 holes (0.094 inch diameter) per square inch in a staggered pattern, which made its area 33 percent open. The spanwise porous strips were obtained by covering the remaining portions of the perforated sheet with a nonporous tape approximately 0.003 inch thick.

The chordwise extent of the porous region on the control surface was selected on the basis of obtaining a suction pressure in the duct sufficiently lower than the surface pressures to insure an inflow velocity variation of no more than ±10 percent along the span of the flap. The width selected was 0.54 inch. The average inflow velocity (both surfaces) was about 100 feet per second at $M = 1.0$. Three chordwise positions of the center line of the porous region were selected: 77.3-, 86.6-, and 95.7-percent wing chord. The porous strip at 77.3-percent chord is illustrated in figure 7(a). For a basis of comparison the completely taped flap was also tested.

An airtight flexible coupling, detailed in figure 5, joined the control surface duct to the wing duct over the entire flap span. Since the test method involved only pressure measurements obtained during forced oscillation of known frequency and amplitude, restraining forces exerted by the coupling had no effect on the results.

Air was drawn through the porous region into the hollow spar in the model and then through a ducting system by the vacuum pumps located outside the test chamber. The exhaust from the pumps was discharged into the plenum chamber surrounding the test section in order to reduce the pressure ratio across the pumps. The quantity of air flowing through the duct system was measured by means of a standard A.S.M.E. orifice.

The control surface was also equipped with spoilers on both sides located at 82-percent wing chord (fig. 7(b)). The spoiler was 0.3 inch in height corresponding to a height to chord ratio of 0.006 at midspan. For this arrangement, the perforated sections of the flap were completely taped.

SCOPE OF TESTS

Sectional flutter derivatives for the control surface were obtained for the various configurations for a wing angle of attack of 0° and for a mean angle of control-surface deflection of 0° for a range of Mach numbers from 0.6 to 1.12. The corresponding Reynolds numbers based on mean aerodynamic wing chord varied from 10.4 to 14.8 million. The control surface was oscillated at an amplitude of $\pm 1.08^{\circ}$ at frequencies from 10 to 30 cycles per second. With Mach number and wing angle of attack constant, data were taken for time intervals of about 30 seconds at each frequency. The over-all accuracy of the pressure-cell data is estimated to be 5 percent in magnitude and $\pm 3^{\circ}$ in phase angle. (See ref. 2.)

RESULTS AND DISCUSSION

The sectional flutter derivatives are presented in table I(a) for the completely taped control surface, tables I(b) through I(d) for the suction-strip configurations, and in table I(e) for the spoiler data. Static pressure distributions are tabulated in table II.

All data presented were derived from the lower row of pressure cells located at the 3/8-semispan wing station. Supplemental results of the investigation are in the form of high-speed motion-picture shadowgraphs.

One important feature of transonic control-surface flutter is that the flow field characteristics are not appreciably different as frequency is increased from low to moderate frequencies, say from 1 to 60 cycles per second. For example, study of shadowgraph motion pictures from investigations reported in references 2, 3, and 6 indicate shock-wave patterns which show only minor variations as frequency is increased. One might assume that the magnitude of the derivative is dependent on how far the shock wave moves, while phase angle is dependent on the pressure field and boundary-layer conditions which not only have an effect on phase lag but are undoubtedly important in determining shock-wave excursion. (It should be pointed out that interference effects such as would result from an adjacent surface are excluded from these remarks.) Boundary-layer control offers the possibility of changing flow field characteristics without changing the external contour of a particular configuration, with possible beneficial effects on the flutter problem.

The effects of suction and spoiler addition on the static-pressure distribution of the control-surface model are shown in figure 8. The application of suction accentuates the negative pressure peak at about 50-percent chord while the spoiler increases the pressure ahead of the spoilers. Large discontinuities in pressure coefficient are produced by each configuration in the region of the control surface.

The effects of suction and spoilers on the flutter derivatives are described in relation to figure 9. It may be noted that the application of suction, $c_q = 0.0019$, had a relatively small effect on the magnitude and phase angle of hinge-moment derivative (fig. 9(a)) and on the aerodynamic damping component (fig. 9(b)). Suction appeared actually to reduce damping at subsonic speeds and lower the Mach number for instability. Curves are shown only for one strip location, 86.6 percent. Results for other locations of the suction strip were quite similar and differed only in secondary detail.

In contrast to the results obtained with suction, the spoiler had a pronounced stabilizing effect. Although the magnitude of the derivative $|c_{h_\delta}|$ was almost constant with Mach number, phase angle, θ, had a pronounced shift toward the stable condition (fig. 9(a)). This resulted in the more stable subsonic damping components shown in figure 9(b). It may be noted, however, that the shift in phase angle was not sufficient to maintain stability at supersonic speeds. This result is different from those for a swept wing reported in reference 4, in that similar spoilers were effective in maintaining stability in the supersonic speed range. However, the present control configuration was different in that it had aerodynamic balance whereas the control in reference 4 had mass balance but no aerodynamic balance.

Examination of the shadowgraph picture disclosed that the application of suction was ineffective in altering the shock-wave position or motion during oscillation. However, small disturbance waves did occur along the suction strip. No evidence of pronounced separation could be detected from static pressures so that the removal of a large separated region did not constitute the primary function of suction. It thus seems likely that an extremely large increase in suction capacity would be required to alter the results appreciably.

The effect of the spoiler was striking in that motion of the shock wave along the surface during control-surface oscillation was almost

[redacted]

completely eliminated. This effect is quite similar to that for triangular shaped wedges reported in reference 3 in which shock-wave motion decreased coincident with the delay of instability to a higher Mach number.

Reynolds Number

A brief investigation of the effects of Reynolds number was conducted in the Ames Unitary Plan wind tunnel. Reducing Reynolds number by a factor of 3 resulted in only small changes in the trends and magnitudes of the data for the plain control surface. These results are similar to those in reference 4 in which the effects of Reynolds number for a swept-wing control-surface configuration were found to be small.

Ames Research Center
National Aeronautics and Space Administration
Moffett Field, Calif., Oct. 7, 1959

REFERENCES

1. Moseley, William C., Jr., and Thompson, Robert F.: Effect of Control Trailing-Edge Thickness or Aspect Ratio on the Oscillating Hinge-Moment and Flutter Characteristics of a Flap-Type Control at Transonic Speeds. NACA RM L58B25, 1958.

2. Wyss, John A., Sorenson, Robert M., and Gambucci, Bruno J.: Effects of Modifications to a Control Surface on a 6-Percent-Thick Unswept Wing on the Transonic Control-Surface Flutter Derivatives. NACA RM A58B04, 1958.

3. Wyss, John A., Sorenson, Robert M., and Gambucci, Bruno J.: Measurements of Transonic Flutter Derivatives for a Midspan Control Surface on a Modified Delta Wing. NASA TM X-157, 1959.

4. Herr, Robert W., Gibson, Frederick W., and Osborne, Robert S.: Some Effects of Flow Spoilers and of Aerodynamic Balance on the Oscillating Hinge Moments for a Swept Fin-Rudder Combination in a Transonic Wind Tunnel. NACA RM L58C28, 1958.

5. Gambucci, Bruno J., and Wyss, John A.: Experimental Investigation of the Drag Due to Wedges Along the Trailing Edge of a Swept Wing. NACA RM A58D15, 1958.

6. Erickson, Albert L., and Stephenson, Jack D.: A Suggested Method of Analyzing for Transonic Flutter of Control Surfaces Based on Available Experimental Evidence. NACA RM A7F30, 1947.

A320

TABLE I.- MEASURED TRANSONIC CONTROL-SURFACE FLUTTER DERIVATIVES

(a) Flap surface taped

M	ω	k	$\lvert c_{h_\delta} \rvert$	θ, deg	$kc_{h_{\dot{\delta}}}$
0.60	62.8	0.199	0.109	180	-0.066
	125.7	.398	.170	186	-.020
	157.1	.497	.100	201	-.040
.70	62.8	.170	.135	180	-.041
	125.7	.341	.085	188	-.025
	157.1	.426	.136	201	-.065
.80	62.8	.151	.268	182	-.027
	125.7	.303	.235	194	-.063
	157.1	.379	.250	195	-.092
.90	62.8	.136	.287	180	-.024
	125.7	.272	.308	190	-.092
	157.1	.340	.289	187	-.068
.92	62.8	.134	.418	181	-.088
	125.7	.268	.373	186	-.072
	157.1	.335	.362	184	-.054
.94	62.8	.128	.582	160	.156
	125.7	.257	.519	160	.144
	157.1	.321	.473	159	.125
.96	62.8	.129	.582	163	.161
	125.7	.259	.544	155	.173
	157.1	.323	.485	157	.144
.98	62.8	.127	.679	159	.173
	125.7	.254	.555	155	.201
	157.1	.317	.541	155	.190
1.00	62.8	.124	.653	159	.165
	125.7	.247	.560	155	.202
	157.1	.309	.587	156	.185
1.05	62.8	.118	.730	161	.178
	125.7	.237	.660	160	.167
	157.1	.296	.716	157	.222
1.09	62.8	.114	.637	163	.121
	125.7	.229	.622	161	.159
	157.1	.286	.619	160	.145

(b) Suction strip at 77.3-percent chord, $c_q = 0.002$

M	ω	k	$\lvert c_{h_\delta} \rvert$	θ, deg	$kc_{h_{\dot{\delta}}}$
0.80	62.8	0.153	0.335	177	-0.007
	125.7	.306	.282	192	-.088
	157.1	.382	.303	196	-.107
.85	62.8	.145	.298	175	-.013
	125.7	.289	.288	190	-.080
	157.1	.362	.330	191	-.083
.90	62.8	.137	.351	178	-.018
	125.7	.273	.404	185	-.058
	157.1	.342	.417	181	-.041
.92	62.8	.134	.412	173	0
	125.7	.268	.456	175	.005
	157.1	.335	.454	169	.050
.94	62.8	.131	.628	166	.114
	125.7	.263	.520	157	.166
	157.1	.329	.557	158	.160
.96	62.8	.129	.670	159	.183
	125.7	.257	.537	155	.186
	157.1	.321	.541	157	.219

(c) Suction strip at 86.6-percent chord, $c_q = 0.002$

M	ω	k	$\lvert c_{h_\delta} \rvert$	θ, deg	$kc_{h_{\dot{\delta}}}$
0.85	62.8	0.144	0.264	180	-0.007
	125.6	.288	.294	188	-.044
	157.0	.360	.288	194	-.101
.90	62.8	.137	.277	180	-.032
	125.6	.273	.346	187	-.047
	157.0	.341	.341	186	-.057
.92	62.8	.134	.351	180	.006
	125.6	.267	.406	180	0
	157.0	.334	.386	180	0
.94	62.8	.131	.666	162	.115
	125.6	.263	.401	162	.142
	157.0	.328	.418	161	.109
.95	62.8	.130	.563	163	.107
	125.6	.261	.502	161	.134
	157.0	.326	.491	163	.127
.96	62.8	.128	.590	160	.180
	125.6	.256	.488	159	.164
	157.0	.320	.472	159	.157
.98	62.8	.126	.623	158	.178
	125.6	.251	.536	155	.188
	157.0	.314	.503	156	.203
1.00	62.8	.124	.698	159	.190
	125.6	.247	.597	157	.197
	157.0	.309	.581	158	.177

(d) Suction strip at 95.7-percent chord, $c_q = 0.002$

M	ω	k	$\lvert c_{h_\delta} \rvert$	θ, deg	$kc_{h_{\dot{\delta}}}$
0.80	62.8	0.156	0.250	180	-0.027
	125.6	.312	.274	188	-.062
	157.1	.390	.531	188	-.071
.90	62.8	.138	.339	180	0
	125.6	.275	.328	214	-.142
	157.1	.344	.315	193	-.075
.95	62.8	.130	.551	159	.093
	125.6	.260	.486	152	.155
	157.1	.326	.250	162	.076
.98	62.8	.126	.686	158	.200
	125.7	.253	.485	146	.216
	157.1	.316	.485	142	.270
.99	62.8	.125	.585	154	.212
	125.7	.250	.487	150	.204
	157.1	.313	.476	147	.209
1.00	62.8	.124	.594	154	.228
	125.7	.249	.505	149	.212
	157.1	.311	.476	151	.213
1.05	62.8	.119	.527	156	.170
	125.7	.238	.456	150	.186
	157.1	.297	.476	150	.164
1.085	125.7	.231	.461	151	.143
	157.1	.288	.452	158	.093
1.09	62.8	.115	.506	160	.167

[redacted]

TABLE I.- MEASURED TRANSONIC CONTROL-SURFACE FLUTTER DERIVATIVES - Concluded

(e) Spoiler at 82-percent chord

M	ω	k	$\lvert c_{h_\delta} \rvert$	θ, deg	$kc_{h_{\dot{\delta}}}$
0.80	62.8	0.155	0.313	186	-0.074
	125.7	.310	.324	199	-.065
	157.1	.387	.341	180	-.153
.85	62.8	.145	.289	188	-.084
	125.7	.290	.266	208	-.097
	157.1	.363	.377	215	-.151
.90	62.8	.137	.302	197	-.060
	125.7	.274	.256	226	-.114
	157.1	.342	.303	180	-.158
.92	62.8	.134	.253	196	-.091
	125.7	.267	.274	227	-.131
	157.1	.334	.294	219	-.149
.94	62.8	.131	.272	202	-.087
	125.7	.262	.275	212	-.121
	157.1	.327	.310	207	-.116
.96	62.8	.128	.304	201	-.108
	125.7	.256	.287	195	-.078
	157.1	.320	.314	197	-.086
.98	62.8	.125	.336	182	-.075
	125.7	.251	.312	171	.011
	157.1	.314	.317	175	.005
1.00	62.8	.123	.402	166	.066
	125.7	.247	.303	159	.078
	157.1	.308	.306	161	.068
1.05	62.8	.118	.438	161	.096
	125.7	.236	.322	162	.066
	157.1	.295	.327	163	.064
1.10	62.8	.113	.493	162	.100
	125.7	.227	.381	163	.075
	157.1	.283	.352	162	.072

[redacted]

TABLE II.- MEASURED PRESSURE DISTRIBUTION FOR THE 5/8-SEMISPAN SECTION; $\delta = 0$

(a) Flap surface taped

Chordwise station, percent chord	Mach number						
	0.90	0.92	0.94	0.96	0.98	1.00	1.05
	Pressure coefficient, c_p						
5	0.073	0.075	0.120	0.105	0.126	0.153	0.215
15	-.196	-.191	-.152	-.169	-.150	-.113	-.058
25	-.206	-.204	-.178	-.196	-.193	-.171	-.122
37.5	-.211	-.250	-.138	-.260	-.248	-.234	-.185
45	-.231	-.226	-.211	-.243	-.229	-.214	-.165
55	-.278	-.300	-.150	-.346	-.349	-.338	-.293
62.5	-.155	-.227	-.212	-.196	-.229	-.355	-.321
67.5	-.176	-.204	-.219	-.234	-.202	-.303	-.357
70.6	-.168	-.178	-.173	-.304	-.376	-.415	-.425
71.9	-.185	-.292	-.191	-.322	-.378	-.415	-.427
74.6	-.021	.029	.060	-.150	-.266	-.325	-.288
80.1	0	0	.057	.009	-.081	-.235	-.295
85.4	-.016	-.010	.033	.009	-.017	-.066	-.313
89.2	.184	-.175	-.143	-.175	-.179	-.215	-.460
93.0	.086	.088	.132	.105	.100	.077	-.128
95.9	.122	.125	.172	.148	.138	.124	.009

(b) Spoiler located at 81.8-percent span

Chordwise station, percent chord	0.90	0.92	0.94	0.96	0.98	1.00	1.05
5	0.073	0.083	0.095	0.110	0.133	0.154	0.200
15	-.191	-.190	-.182	-.169	-.147	-.113	-.069
25	-.201	-.204	-.205	-.196	-.190	-.176	-.138
37.5	-.211	-.248	-.260	-.285	-.272	-.235	-.193
45	-.216	-.229	-.248	-.262	-.246	-.216	-.174
55	-.221	-.287	-.285	-.245	-.234	-.342	-.304
62.5	.082	-.092	-.181	-.393	-.351	-.356	-.334
67.5	.082	-.092	-.124	-.187	-.298	-.325	-.365
70.6	-.052	.005	-.030	-.047	-.162	-.217	-.341
71.9	-.064	-.013	-.041	-.056	-.166	-.219	-.341
74.6	.125	.131	.146	.070	-.067	-.165	-.244
80.1	.237	.238	.248	.212	.101	.018	-.009
85.4	-.480	-.496	-.505	-.473	-.388	-.361	-.443
89.2	-.382	-.401	-.410	-.383	-.395	-.397	-.495
93.0	-.062	-.063	-.051	-.028	-.023	-.051	-.182
95.9	.018	.013	.026	.044	.050	.027	-.082

[redacted]

TABLE II.- MEASURED PRESSURE DISTRIBUTION FOR THE 5/8-SEMISPAN SECTION; δ = 0 - Continued

Chord-wise station, percent chord	Mach number					
	0.90	0.92	0.94	0.96	0.98	1.00
	Pressure coefficient, c_p					
(c) Suction strip at 77.3-percent span, c_q = 0.002						
5	0.080	0.096	0.115	0.137		
15	-.199	-.191	-.171	-.146		
25	-.209	-.224	-.196	-.185		
37.5	-.266	-.285	-.259	-.249		
45	-.236	-.253	-.237	-.227		
55	-.298	-.299	-.325	-.333		
62.5	-.262	-.262	-.190	-.202		
67.5	-.239	-.274	-.229	-.205		
70.6	-.216	-.254	-.380	-.408		
71.9	-.234	-.283	-.395	-.408		
74.6	-.010	-.011	-.233	-.322		
80.1	.067	.096	.087	-.071		
85.4	.047	.052	.068	.022		
89.2	.041	.038	.068	.019		
93.0	.089	.104	.112	.107		
95.9	.149	.158	.168	.160		
(d) Suction strip at 86.6-percent span, c_q = 0.002						
5	0.078	0.096	0.124	0.131	0.063	0.192
15	-.198	-.195	-.167	-.154	-.171	-.088
25	-.208	-.218	-.193	-.106	-.275	-.146
37.5	-.266	-.283	-.276	-.262	-.340	-.226
45	-.234	-.254	-.257	-.240	-.313	-.211
55	-.300	-.285	-.353	-.355	-.340	-.184
62.5	-.256	-.258	-.267	-.224	-.405	-.310
67.5	-.234	-.274	-.276	-.210	-.343	-.336
70.6	-.181	-.224	-.343	-.382	-.414	-.415
71.9	-.198	-.246	-.356	-.379	-.515	-.417
74.6	.023	.019	-.194	-.290	-.414	-.300
80.1	-.044	-.020	-.067	-.151	-.400	-.313
85.4	-.063	-.053	-.062	-.115	-.324	-.318
89.2	.073	.085	.086	.070	-.076	-.060
93.0	.106	.117	.133	.131	.010	.088
95.9	.150	.164	.172	.169	.056	.143

[redacted]

TABLE II.- MEASURED PRESSURE DISTRIBUTION FOR THE 5/8-SEMISPAN SECTION; $\delta = 0$ - Concluded

(e) Suction strip at 95.7-percent span, $c_q = 0.002$

Chordwise station, percent chord	Mach number				
	0.90	0.95	0.98	1.00	1.05
	Pressure coefficient, c_p				
5	0.077	0.120	0.158	0.180	0.218
15	-.200	-.168	-.120	-.093	-.043
25	-.209	-.205	-.184	-.166	-.104
37.5	-.259	-.271	-.248	-.230	-.174
45	-.229	-.251	-.220	-.207	-.148
55	-.298	-.349	-.347	-.334	-.277
62.5	-.238	-.192	-.350	-.358	-.304
67.5	-.219	-.226	-.285	-.388	-.343
70.6	-.179	-.341	-.340	-.430	-.414
71.9	-.199	-.348	-.349	-.433	-.417
74.6	.023	-.206	-.256	-.324	-.278
80.1	-.011	-.059	-.227	-.316	-.310
85.4	-.005	-.009	-.073	-.298	-.286
89.2	.010	.014	-.039	-.153	-.273
93.0	.093	.056	-.037	-.072	-.251
95.9	.157	.162	.157	.081	-.194

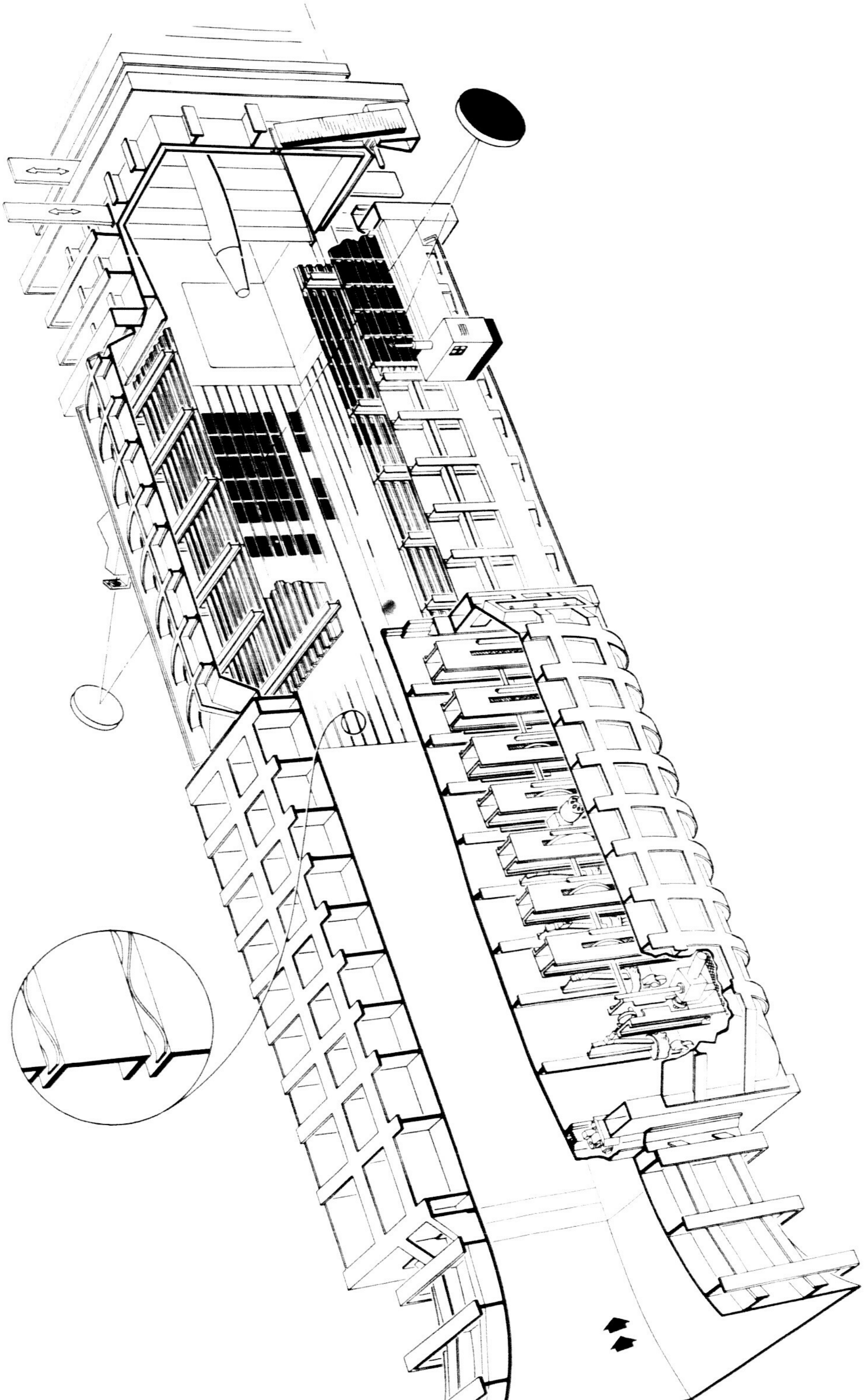

Figure 1.- Sectional sketch of the nozzle and test section of the Ames 14-foot transonic wind tunnel.

A-24146

Figure 2.- Rear view of model mounted in test section.

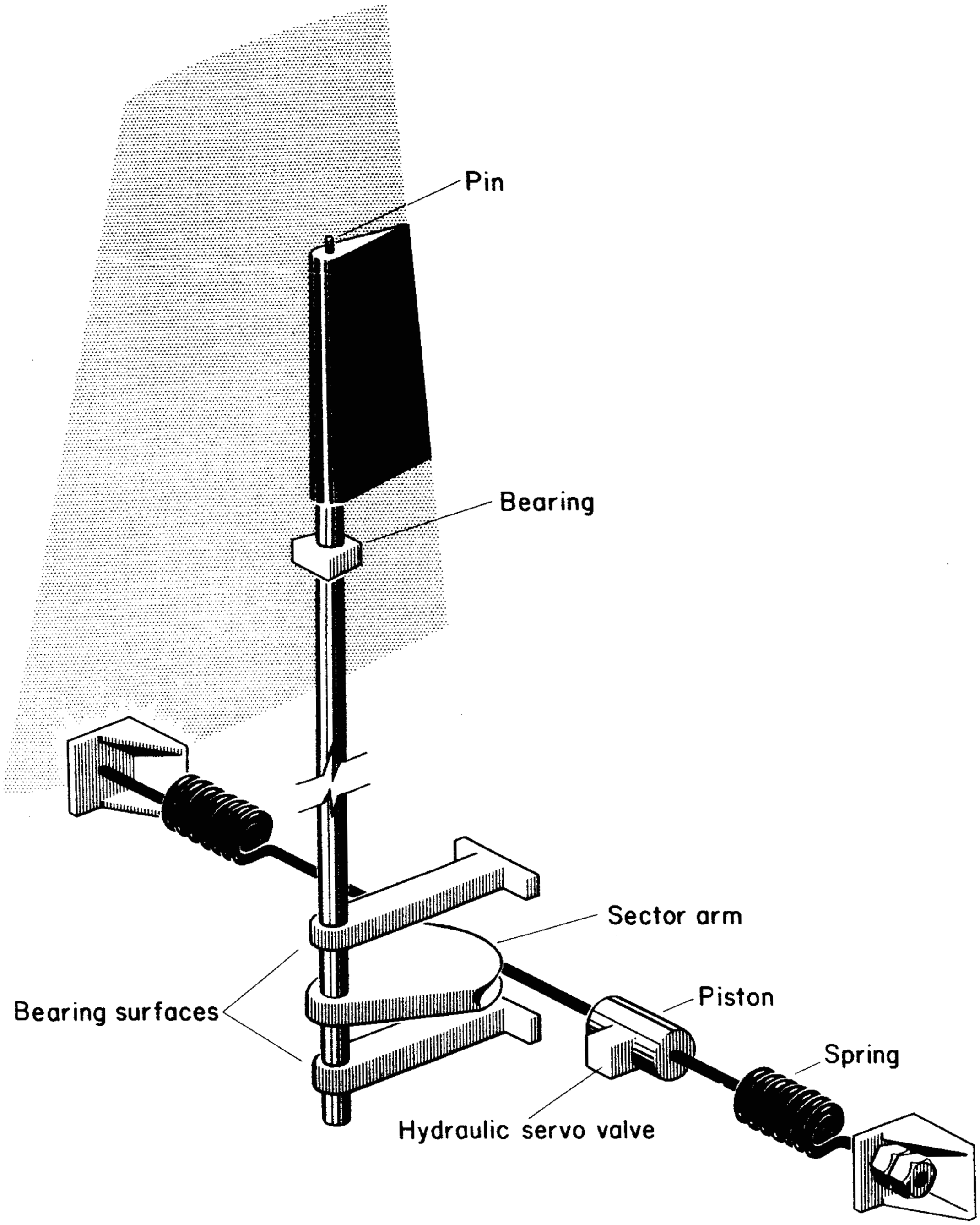

Figure 3.- Schematic drawing of the control-surface drive system.

[redacted]

[redacted]

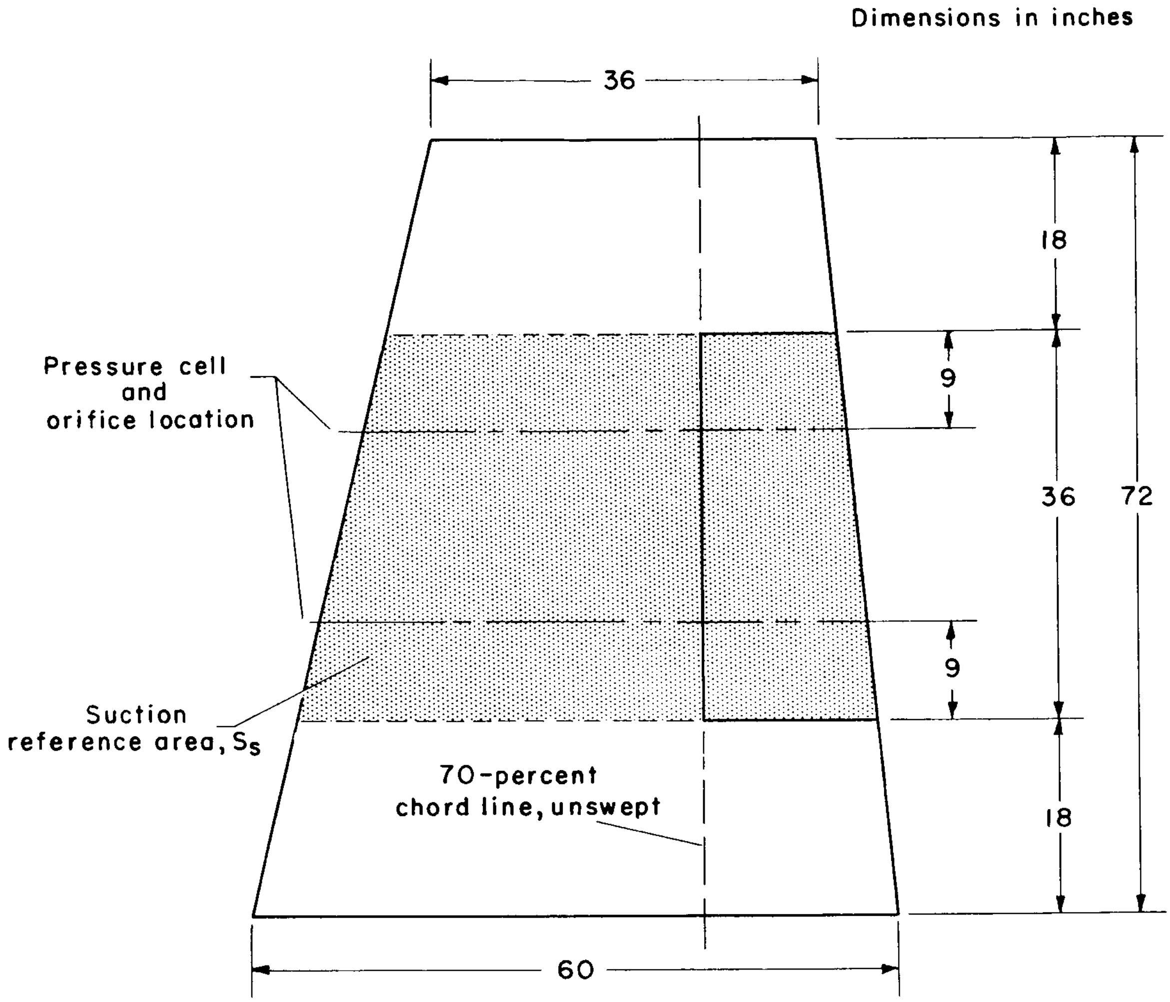

Figure 4.- Dimensional sketch of model plan form.

[redacted]

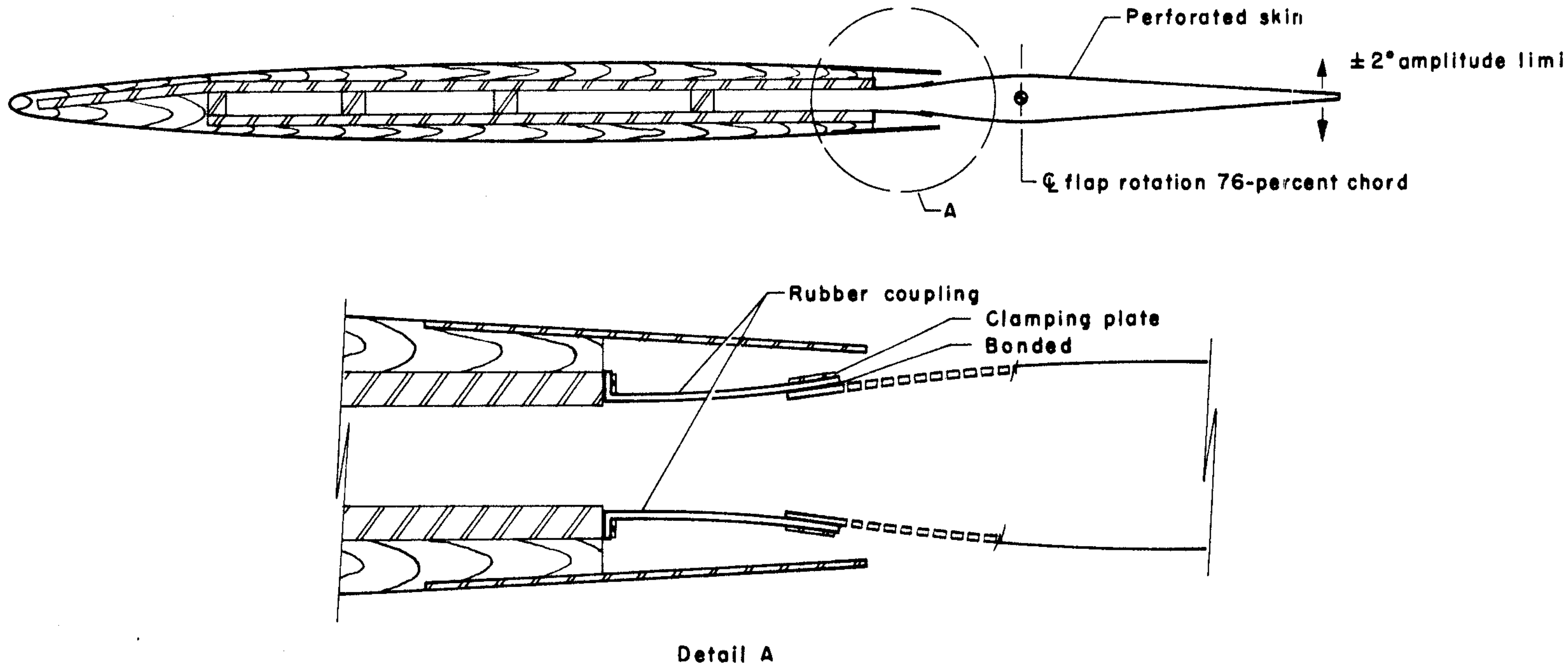

Figure 5.- Cross section of model at the control surface.

[redacted]

DECLASSIFIED

[redacted]

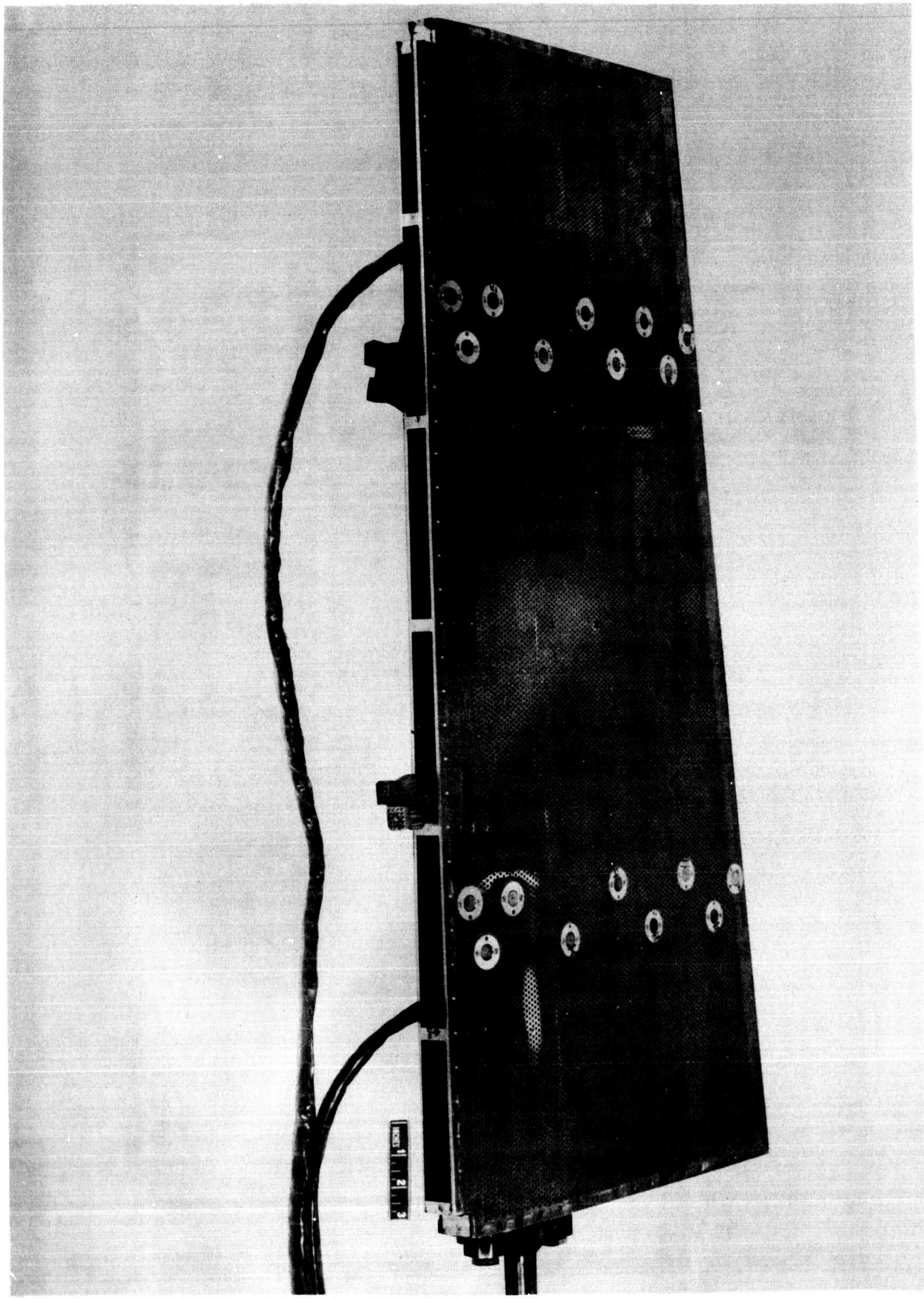

Figure 6.- Control surface.

A-24031.1

[redacted]

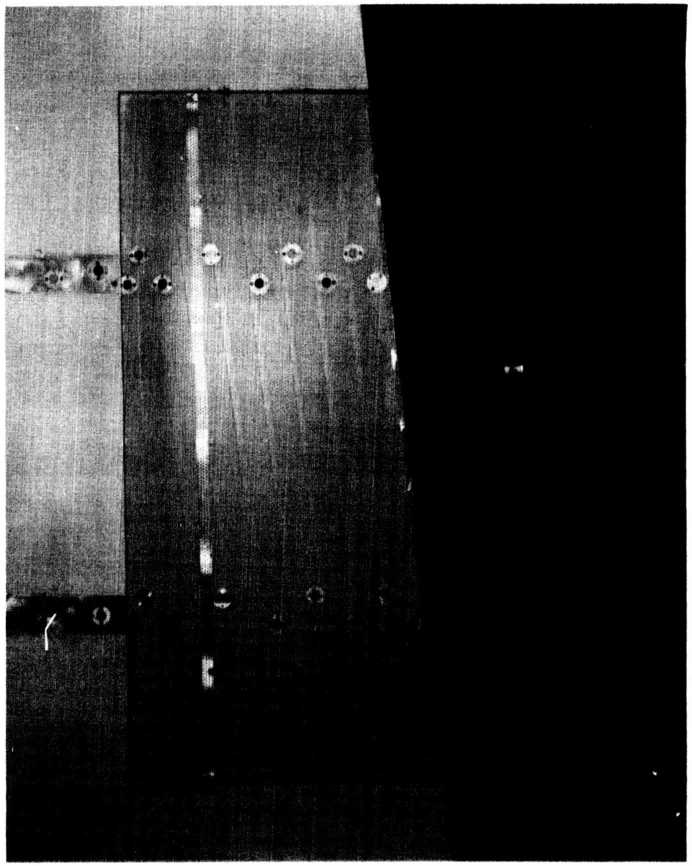

A-24206

(a) Suction strip at 77.3-percent chord.

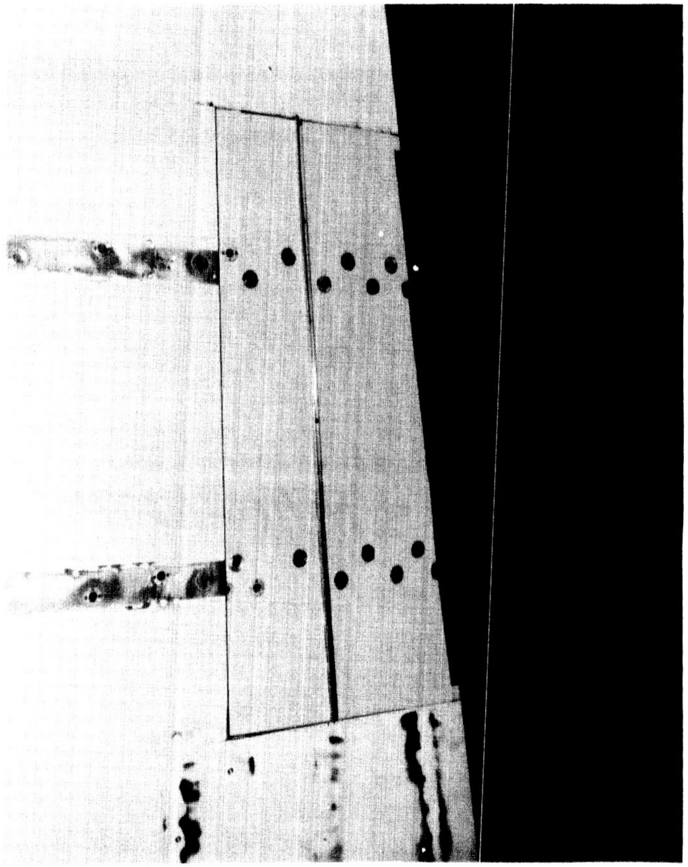

A-24194

(b) Spoiler mounted at 82-percent chord.

Figure 7.- Views of suction and spoiler configurations.

DECLASSIFIED [redacted]

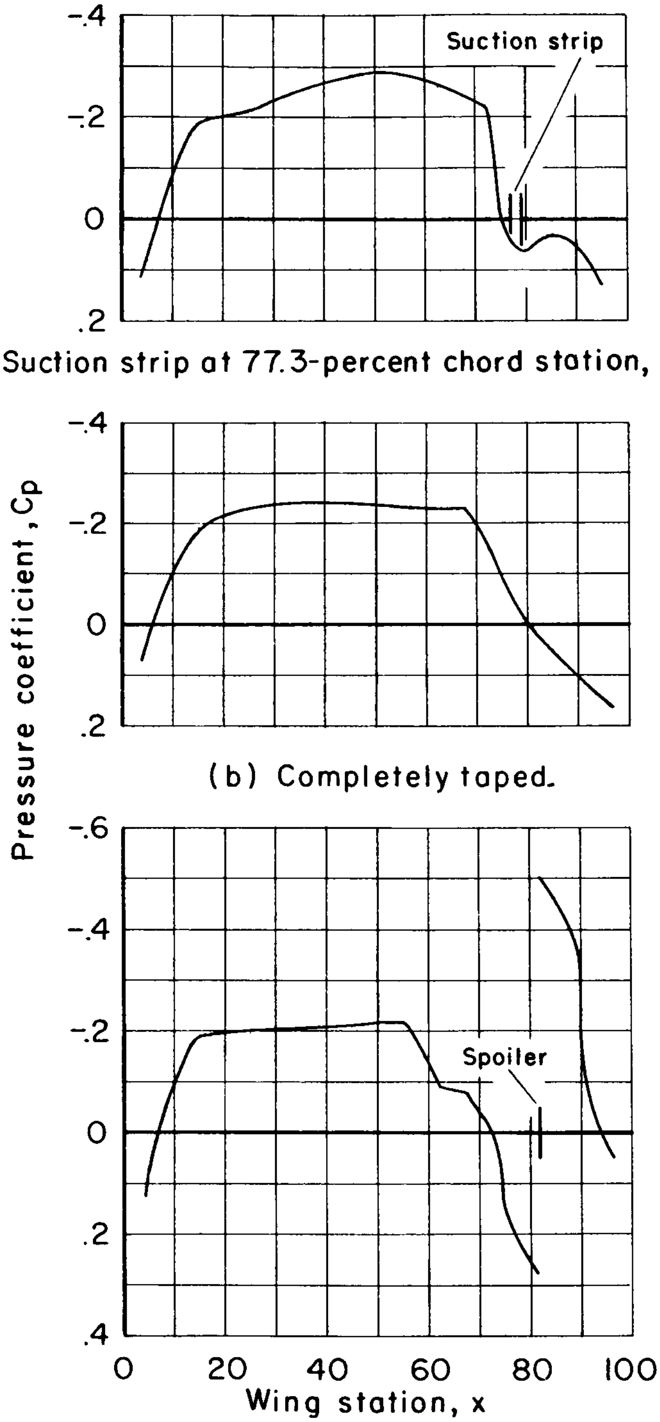

(a) Suction strip at 77.3-percent chord station, c_q =.0019.

(b) Completely taped.

(c) Spoilers at 82-percent chord station.

Figure 8.- Wing and control-surface static pressure coefficients, M = 0.90.

[redacted]

[redacted]

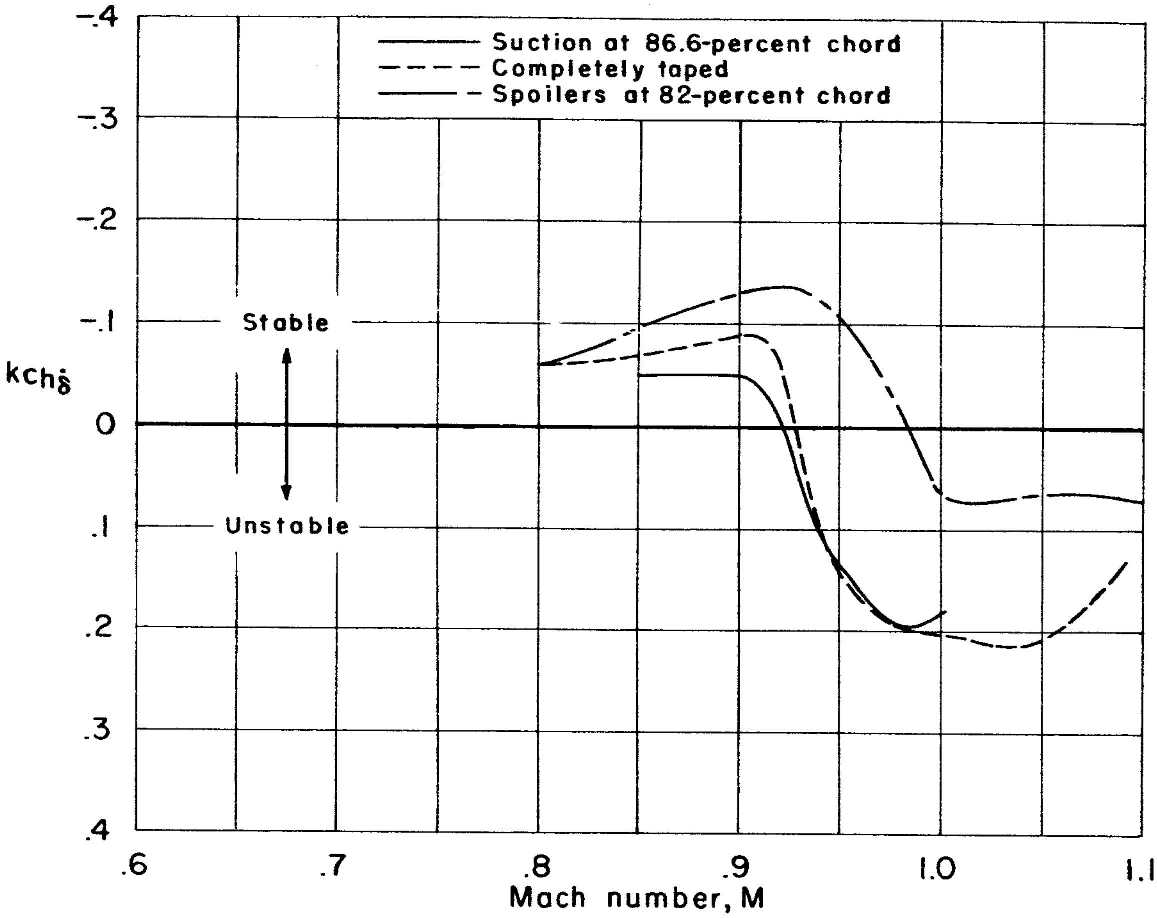

(b) Aerodynamic damping component as a function of Mach number.

Figure 9.- Concluded.

[redacted]

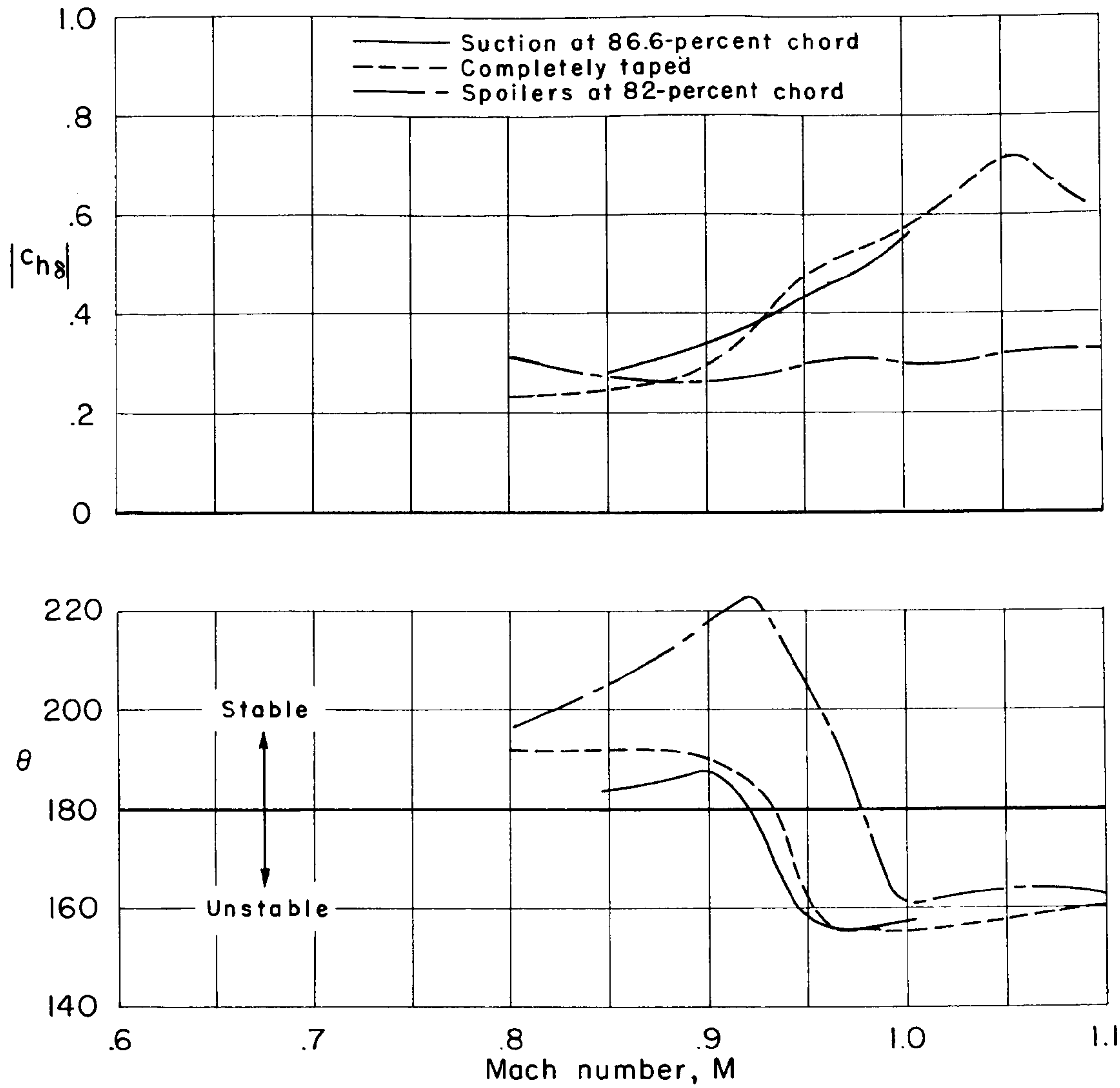

(a) Resultant aerodynamic hinge moment and phase angle as functions of Mach number.

Figure 9.- Results for suction, taped, and spoiler configurations; $k = 0.3$, $c_q = 0.0019$.